Parameter ranges should be chosen wide enough to include all plausible values for the given case, even if their probability is low. We also assume that for some parameters it was possible to give an initial guess p_k^0 as well as choose an a-priori probability distribution function. For example, the normal distribution $p_k \sim N(p_k^0, \sigma_k)$ can be assumed (Fig. 2), where a modeller provides an appropriate deviation estimate σ_k. The higher the certainty of the initial guess p_k^0, the lower the deviation σ_k.

2.2 Optimization Problem

In order to identify the parameter vector p that fits the monitoring data, a constrained optimization problem is defined to minimize the error between the monitored and simulated energy demand:

$$\min J(p), \quad \text{where } p_k \in [p_k^{min}, p_k^{max}] \qquad (1)$$

In order to optimally represent the building under consideration, the cost function should also include an a-priori knowledge on the parameter probability. Hence, the cost function $J(p)$ is designed as summation of the cumulative absolute simulation error for temperature and heating demand, and a regularization term representing penalization depending on parameter probability:

$$J(p) = \sum_{j=1}^{N}\left(w_T\left|T_j^m - T_j^s\right| + w_Q\left|Q_j^m - Q_j^s\right|\right) + \sum_{k=1}^{N} w_k\ f_{pen,k}(p_k). \qquad (2)$$

Here, T and Q denote indoor air temperature and cumulative heating demand, respectively. Superscripts m and s represent measured and simulated values respectively, and subscript j denotes the corresponding value at the j[th] time step. Since scales for the temperature and heat demand vary largely, the corresponding error terms should be balanced using appropriate weights w_T and w_Q. However, since the goal of the calibration is to accurately predict the heating demand, the corresponding error should still be dominant. Adding a regularization term can be interpreted as imposing certain a-priori distributions on model parameters. Here $f_{pen,k}(p_k)$ and w_k denote the penalty function and weight for each parameter p_k. The penalty term $f_{pen,k}$ should increase as $|p_k - p_k^0|$ increases, i.e. when parameter p_k takes less probable values. For this reason let

$$f_{pen,k}(p_k) = \widetilde{f}_{pen,k}(|p_k - p_k^0|) \qquad (3)$$

such that $\widetilde{f}_{pen,k} : \mathbb{R}^+ \to \mathbb{R}^+$ is a monotonically increasing function. Hence, it could be defined as (Fig. 2):

$$f_{pen,k}(p_k) = \frac{1}{\sqrt{2\,\sigma_k{}^2}}\left(1 - e^{-\frac{(p_k - p_k^0)^2}{2\,\sigma_k^2}}\right). \qquad (4)$$

Since the penalty term not necessarily needs to be defined as a weighted norm, it represents a generalization of the Tikhonov regularization. The problem (1) can be observed as a multi-objective optimization problem, where a trade-off is made between minimizing the simulation error and maximizing the parameter probability.

3. Study Case Model Calibration

In this section, the methodology introduced in Section 2 is illustrated on a residential building apartment model. The presented results offer evidence of regularization benefits on the retrofit prediction and model parameter estimation.

3.1 Study Case Description

The residential building under consideration is located in the south of Madrid, Spain. Built in the 1960s, with poorly fitted windows, no insulation and cracks around doors, windows, and foundations, it was deemed suitable for retrofit. On the eastern side, it is attached to a twin residential building (Fig. 3).

Fig. 3 – Study case residential building

Each block contains five 50 m[2] apartments. The study case apartment is located in the west block on the last floor (Fig. 4).

It used a gas boiler with five water radiators for the heating in winter and a split unit for the cooling in summer. Monitoring data is available for one year before the retrofit (September 2014 — September 2015), and two months after the installation of new windows and insulation layers on the envelope (January 2016 – March 2016).

The acquired real-time data with 15 min samplings include internal (IAT) and external (EAT) temperatures, global solar radiation, CO_2 concentration, and electric consumption. A heat meter on supply and return pipes of the gas boiler was also installed to monitor the heating energy. The heating demand at each time step is easily calculated as the increase in the measurement of heating energy. The internal temperature of the apartment below was monitored as well, but not the one of the apartment adjacent on the eastern side.

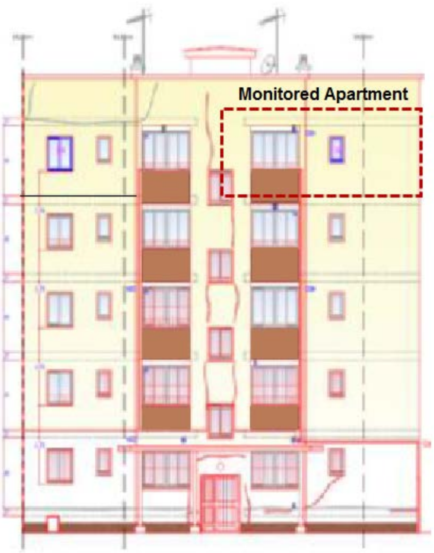

Fig. 4 – Front view

3.2 Initial Building Energy Model

The initial energy model for the whole building was developed in the dynamic environment of TRNSYS Simulation Studio (Klein et al., 2010), where the building geometry was developed in Google SketchUp and set up in TRNBuild. The model is based on the information provided by the energy audit (Garcia et al., 2014), including building plans, envelope structure, openings, air tightness, internal partitions, shading elements, and occupancy. Each apartment is divided in two thermal zones, north and south oriented (see Fig. 5). Since the heating setpoint of the apartment is unknown, we assume an ideal heating. An infiltration coefficient is used when the windows are closed, and another when windows are open. Internal heat gains from occupants and equipment are included, where 75 W/person is assumed and heat gain from electric appliances is estimated based on real-time electric meter measurements and guidelines by ASHRAE (1985). The shading model is based on an on/off differential controller that takes into account the indoor air temperature and solar irradiance at each window according to its orientation. Shading is activated when both indoor temperature and solar irradiance on horizontal plane exceed a certain threshold. The threshold for the temperature controller is equal to the calibration parameter p_4, and 250 W is chosen for the solar irradiance controller. The external shading factor is the calibration coefficient p_3 taken to be the same for all windows in the apartment. The new control value for each controller is the output control signal from the previous time step, by introducing a hysteresis effect. Therefore, both lower and upper deadband for the difference between actual and threshold values, also need to be defined. These deadbands are chosen to be -0.5 °C and 0.5 °C for the temperature controller, and -50 W and 0 W for the solar radiation controller. The shading activation is an adaptation of the controller values defined by Dott et al. (2013).

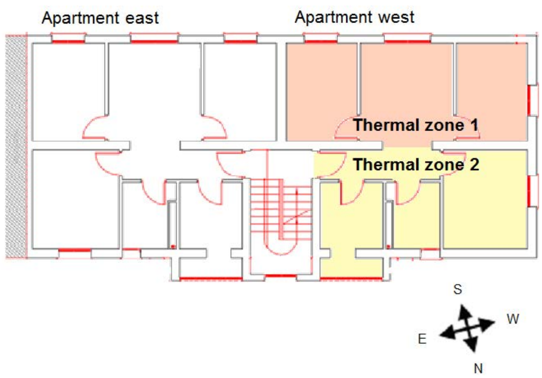

Fig. 5 – Building cross-section

The sensitivity analysis was performed using the Morris method (Saltelli, 2008), and significant model parameters for the energy demand assessment were identified (Table 1).

Table 1 – Significant model parameters

Parameter	Description [Unit]
p_1	Internal temperature of the adjacent apartment [°C]
p_2	Occupancy multiplication factor [-]
p_3	Shading factor [-]
p_4	Shading activation temperature [°C]
p_5	Infiltration with windows closed [ACH]
p_6	Total infiltration and ventilation with windows open [ACH]
p_7	Conductivity of the concrete layer in the external walls [W/(m K)]
p_8	Conductivity of the concrete layer in the internal partitions, floors and ceilings [W/(m K)]
p_9	Conductivity of the concrete layer in the roof [W/(m K)]
p_{10}	Window U-value [W/(m^2 K)]

The outcome shows that the IAT of the adjacent apartments (p_1) has a strong influence on the heat demand. Parameter p_2 represents the correction factor for the assumed occupant's heat gain. In addition, the parameters of the shading model (p_3, p_4) are mostly significant in the summer and swing period. Infiltration parameters (p_5, p_6) turn out to have a strong effect on both IAT and heat demand, as expected. To account for possible errors in layer description of the external and internal walls, floor and roof, and the fact that walls are reinforced, we have included the conductivity of the concrete as uncertain model parameters (p_7, p_8 and p_9). Parameter p_{10} represents the windows U-value. Since for a number of apartments in the building, additional windows were already installed, we want to prove our hypothesis that the monitored apartment has double windows. As an initial point, minimum and maximum values of each parameter were defined (Table 2), based on the energy audit and by consulting various standards and datasheets.

Table 2 – Parameter range and initial guess

Parameter	p_k^{min}	p_k^{max}	p_k^0	σ_k
p_1	17.6	24.6	18.6	-
p_2	0.5	2	1	0.3
p_3	0	1	0.5	-
p_4	22	32	25	-
p_5	0.15	0.75	0.4	0.6
p_6	0.4	5.2	3	-
p_7	0.8	2.5	1.13	0.35
p_8	0.8	2	1.13	0.35
p_9	0.8	2	1.13	0.45
p_{10}	2.74	5.68	2.83	-

In particular, the initial guess for the infiltration parameter (p_5) is based on the blower-door test which was performed during the energy audit (Table 3).

Table 3 – Blower-doors test results

ΔP [Pa]	Flow [m^3/h]	ACH
20	200	2.0
30	276	2.8
50	382	3.9
65	471	4.7

The airflow through the building envelope and the pressure difference across it are known to have the following relationship (Sherman, 1987):

$$q = \mathrm{C}\,(\Delta \mathrm{P})^{n} \tag{5}$$

Here ΔP is the induced pressure difference (in Pa), q is the airflow through the building envelope (in m^3/h), and C is the air leakage coefficient. To determine the parameters n and C, the least-square technique is applied to the blower-door test results following ISO standard (ISO/TC 163/SC 1, 2015). The reached values $n = 0.67$ and $C = 260$ have a standard deviation estimate 0.02 and 3 respectively, and $r^2 = 99.7$ %. In order to estimate the average air infiltration, stack-dominated and wind-dominated components are evaluated separately (Klems, 1983). From one year measurement data, the average indoor air temperature, the temperature difference between the indoor and external air, and the air density were obtained and used to calculate the average stack effect pressure difference to be $\Delta P_{se} = 1.03$ Pa. From the meteorological data, the average wind speed in Madrid is estimated to be 2 m/s, implying a wind pressure difference equal to $\Delta P_w = 1.23$ Pa. Hence, the stack effect air infiltration and the infiltration due to the wind are equal to 0.3 ACH and 0.27 ACH respectively, which implies an infiltration rate of 0.4 ACH (Klems, 1983). The occupancy multiplication parameter p_1 is estimated to be equal one, where we assume that 75 W/person provided by ASHRAE (1985) is a well-studied approximation. The conductivity of the concrete found in the walls, floors and partitions (p_8, p_9 and p_{10}) is provided by the refurbishment architect during the energy audit (Garcia et al., 2014). These initial guesses are considered reliable and are assigned a divergence factor. The corresponding penalty is added to the cost function of the optimization problem. The window U-value and the shading coefficient are estimated with less certainty by inspecting the windows and the indoor temperature. Since ventilation rates with open windows (p_6) cannot be easily estimated, a wide parameter range was chosen and the approximate mean value was selected as the initial guess. Initial guesses that are not reliable are not included in the regularization term.

3.3 Calibration and Validation Procedure

The monitoring data was divided into three periods: the calibration period (September 11, 2014–January 31, 2015), and the validation period before (February 01, 2015–April 12, 2015) and after the renovation (January 21, 2016–March 29, 2016). Opening of the windows and occupancy in the apartment were identified on the basis of CO2 levels. Measured IATs were set as the heating setpoint in the monitored apartment and for the apartment below. However, the IAT measurement is not available for the apartment adjacent on the eastern side, which is therefore treated as an unknown model parameter (p_1). Although the whole building is simulated, the results for the monitored apartment were considered just in the cost function. The heating demand and the average indoor air temperature during the heating season are summarized in Table 4.

Table 4 – Monitoring data summary

Period	Heat demand [kWh]	Average heating IAT [°C]
Calibration	3755	21.91
Validation 1	2252	21.76
Validation 2	1222	22.62

Since the ideal heating is assumed and the IAT is taken as the setpoint, the temperature error is negligible in the heating periods. Therefore, it is included in the cost function only when there is no heating. Used weight coefficients are $w_T = 0.65$ and $w_Q = 5.7e-3$, in order to approximately achieve a 1:4 ratio between temperature and energy demand error. For a regularized solution $w_k = 100$ is taken. As soon as the optimization problem was solved, the models were validated on a new set of monitoring data. Since the average measured heating power was 1.9 kW, the sensor resolution of the heating demand (1 kWh) was not suitable to take into consideration the normalized mean bias (NMB) and the coefficient of variation of root mean square error (CVRMSE) on an hourly basis. Instead, the daily NMB and CVRMSE were reported. The recommended calibration criteria per ASHRAE (2002) for hourly values are NMB ≤±10 % and CVRMSE ≤30 %, and NMB ≤±5 % and CVRMSE ≤15 % for monthly data. However, according to the knowledge of the authors, there are no standard criteria for daily values. Hence, as daily criteria we use a combination of ASHRAE defined criteria: NMB ≤±5 % and CVRMSE ≤15 % for calibration, and NMB ≤±5 % and CVRMSE ≤30 % for validation. For model validation after the renovation, models were adapted to include new windows, the corresponding infiltration parameter and insulation layers, as specified in the manufacturers' datasheets.

3.4 Regularized and Non-Regularized Solution

Hybrid algorithm combining Particle Swarm optimization and Hooke-Jeeves optimization algorithms from GenOpt (Wetter, 2009) were used to solve the optimization problems. Regularized and non-regularized solution models were obtained using the same algorithm parameters and the initial parameter set, solving optimization problem (1), where the cost function (2) in the former case includes also the regularization term. The obtained parameter sets are reported in Table 5. Both models yield zero shading since otherwise the simulated IAT would be much lower than monitored. However, four parameters of the non-regularized model reach boundary values of the pre-defined parameter range. For example, when the windows are open infiltration reaches minimal 0.4 ACH, thus contradictory since it is smaller than the infiltration with windows closed (0.62 ACH).

Table 5 – Calibrated model parameters

Parameter	Regularized	Non-regularized
p_1	18.08	18.6
p_2	1.25	2
p_3	0	0
p_4	28	30
p_5	0.35	0.62
p_6	1.46	0.4
p_7	1.13	0.88
p_8	1.51	1.99
p_9	1.13	1.99
p_{10}	2.74	2.74

We also note that the conductivity of the concrete in internal partitions and roof also reaches the maximum value of the interval. Compared with the regularized solution, these values are significantly larger and result in larger transmission losses through the roof. And also, a larger infiltration when windows are closed results in a larger infiltration loss compared to the regularized solution. These losses are counterbalanced by a higher gain from the occupants (150 W/person, maximum value), a reduced infiltration when windows are closed, and less transmission losses through external walls. The parameters of the non-regularized model that reach minimum or maximum values represent possible, but highly unlikely, scenarios. Table 6 summarizes the calibration results for both models. Both models satisfy the calibration criteria. Also the average absolute error (AAE) for cumulative heat demand and temperature calculated at 15-minute intervals is considered.

$$AAE\ Heat = \frac{\sum_{k=1}^{n} \left| \int_{t_0}^{t_k} (\dot{Q}^s - \dot{Q}^m)\, \mathrm{dt} \right|}{n} \frac{100}{\int_{t_0}^{t_n} \dot{Q}^m\, \mathrm{dt}} \quad (6)$$

$$AAE\ Temp = \frac{\sum_{k=1}^{n} |T_k^s - T_k^m|}{n} \quad (7)$$

$\dot{Q}_{sim}$ and $\dot{Q}_{mea}$ are simulated and measured heating power. Average absolute heating demand error amounts to 0.45 % and 0.34 % of the total measured heating energy demand (3755 kWh, see Table 4) for the regularized and non-regularized solution.

Table 6 – Calibration error (Sep 11, 2014 – Jan 31, 2015)

	Regularized	Non-regularized
NMB	-0.85	-0.47
CVRMSE	9.57	10.3
AAE Heat [kWh]	11.64	12.6
AAE Temp [°C]	1.24	1.09

Table 7 reports the error for both solutions in the validation period before the renovation.

Table 7 – Pre-renovation (Feb 01, 2015 – Apr 12, 2015) validation results

	Regularized	Non-regularized
NMB	-3.97	-3.53
CVRMSE	22.38	22.98
AAE Heat [kWh]	82.12	78.09
AAE Temp [°C]	0.92	0.82

The total measured heating demand for the validation period reads 2252 kWh, and the values predicted by the regularized and the non-regularized solution are 2150 kWh and 2157 kWh, which represents under-prediction of 4.44 % and 4.22 % respectively.

Both models satisfy the validation criteria. The regularized solution has a slightly better performance with respect to NMB and CVRMSE, while the non-regularized solution has lower average absolute errors. The model predictions for the post-retrofit period are given in Table 8. The total monitored heating demand in that period is 1222 kWh. The predictions obtained by regularized and non-regularized solution read 1173.8 kWh and 1099 kWh, hence the models under-predict the demand by 3.9 % and 10.1 %, respectively. The regularized solution yields a better estimate of the building energy demand after the renovation. The non-regularized solution underestimates the heating demand by over 10 % because it overestimates the occupant internal gain, while it underestimates the infiltration losses.

Table 8 – Post-renovation (Jan 21, 2016 – Mar 29, 2016) validation results

	Regularized	Non-regularized
NMB	-3.66	-10.1
CVRMSE	25.3	29.9
AAE Heat [kWh]	19.66	47.9
AAE Temp [°C]	0.89	0.76

4. Discussion and Further Research

We have illustrated how calibrated and validated building models do not necessarily provide good renovation savings estimates. The parameter optimization method for complex building energy models presented in this work aims to reduce the parameter uncertainty and thus the prediction error by utilizing regularization. The proposed method is in general useful when the number of model parameters is large, since the chances to perform a good search of the parameter space by using statistical sampling, is small and the model uncertainty increases. The performance of a guided search of the parameter space instead is advantageous, e.g. it solves a parameter optimization problem.

This work also highlights the importance of a good preliminary estimation of the building parameters; otherwise, unrealistic parameter combinations may emerge as optimal in the calibration phase.

The success of the regularization strongly depends on the choice of the penalty weight in the cost function. How to optimally choose this value has not been considered here and is a topic for further research. A possible approach is to address (1) as a multi-objective optimization problem and evaluate different Pareto optimal solutions. Finally, although only the heating demand was considered, this method naturally extends to the calibration of the models with respect to both the heating and the cooling demand.

Acknowledgement

This study is performed as part of iNSPiRe project, funded by the European Commission's 7th Framework Programme 2007–2013 under GA no. 314461.

Nomenclature

Symbols

C	Air pressure leakage coefficient
$f_k(p_k)$	Penalty function for k[th] parameter
$J(p)$	Cost function
n	Air pressure exponent coefficient
p_k	k[th] model parameter
p	Parameter vector
q	Air flow through building envelope
Q	(Cumulative) Heating demand
$\dot{Q}$	Heating power
T	Indoor Air temperature
w_k	Weight for k[th] parameter p_k penalty function
w_Q	Weight for heating demand error
w_T	Weight for temperature error
ΔP	Induced pressure difference

Subscripts/Superscripts

j	Value at the j[th] time step
m	Monitored value
s	Simulated value
se	Stack-effect dominated value
w	Wind dominated value

References

Alifanov, O.M., E.A. Artiu͡khin, S.V. Rumia͡nt͡sev. 1995. *Extreme methods for solving ill-posed problems with applications to inverse heat transfer problems*. New York, U.S.A.: Begell House.

ASHRAE. 2002. *ASHRAE Guideline 14-2002: Measurement of Energy and Demand Savings*. Atlanta, U.S.A.: American Society of Heating, Refrigerating and Air-Conditioning Engineers.

ASHRAE. 1985. *ASHRAE handbook: Fundamentals*. Atlanta, U.S.A.: American Society of Heating, Refrigerating and Air Conditioning Engineers.

Caucheteux, A., E. Stephan, C. Ouest. 2013. "Transient simulation calibration of an old building using an experimental design: evaluating uncertainty results". In: *Proceedings of the 13th IBPSA Conference*. Chambéry, France: IBPSA.

Coakley, D., P. Raftery, P. Molloy. 2012. "Calibration of whole building energy simulation models: Detailed case study of a naturally ventilated building using hourly measured data". In: *First Building Simulation and Optimization Conference*. Loughborough, UK IBPSA.

Crépey, S. 2003. "Calibration of the Local Volatility in a Generalized Black--Scholes Model Using Tikhonov Regularization". S*IAM Journal on Mathematical Analysis* 34: 1183–1206. doi:10.1137/S0036141001400202

Dott, R., M.Y. Haller, J. Ruschenburg, F. Ochs, J. Bony. 2013. "The Reference Framework for Sys¬tem Simulations of the IEA SHC Task 44/HPP Annex 38 Part B: Buildings and Space Heat Load". In: *A Technical Report of Subtask C, Report C1 Part B*.

Garcia, J., D. Romera, C. Dipasquale, R. Fedrizzi, M. D'Antoni. 2014. "Energy audit – Case study Madrid Development of Systemic Packages for Deep Energy Renovation of Residential and Tertiary Buildings including Envelope and Systems". URL http://www.inspirefp7.eu/wp-content/uploads/2014/07/WP7_D7.1b_20140514_P15_Energy_Audit_Madrid.pdf

Heo, Y., R. Choudhary, G.A. Augenbroe. 2012. "Calibration of building energy models for retrofit analysis under uncertainty". *Energy and Buildings* 47: 550–560. doi:10.1016/j.enbuild.2011.12.029.

ISO. 2015. *ISO/TC 163/SC 1, 2015. ISO 9972:2015: Thermal performance of buildings — Determination of air permeability of buildings — Fan pressurization method*. Geneve, Switzerland: ISO.

Klems, J.H. 1983. "Methods of estimating air infiltration through windows". *Energy and Buildings* 5: 243–252. doi:10.1016/0378-7788(83)90012-9.

Navon, I.M. 1998. "Practical and theoretical aspects of adjoint parameter estimation and identifiability in meteorology and oceanography". *Dynamics of Atmospheres and Oceans* 27, 55–79. doi:10.1016/S0377-0265(97)00032-8.

Raftery, P., M. Keane, J. O'Donnell. 2011. "Calibrating whole building energy models: An evidence-based methodology". *Energy and Buildings* 43: 2356–2364. doi:10.1016/j.enbuild.2011.05.020.

Reddy, T.A., I. Maor, C. Panjapornpon. 2007. "Calibrating Detailed Building Energy Simulation Programs with Measured Data—Part I: General Methodology (RP-1051)". *HVAC&R Research* 13: 221–241. doi:10.1080/10789669.2007.10390952

Saltelli, A. 2008. *Global sensitivity analysis: The primer*. Chichester, UK: John Wiley.

Schirrer, A., M. Brandstetter, I. Leobner, S. Hauer, M. Kozek. 2016. "Nonlinear model predictive control for a heating and cooling system of a low-energy office building". *Energy and Buildings* 125; 86–98. doi:10.1016/j.enbuild.2016.04.029.

Sherman, M.H. 1987. "Estimation of infiltration from leakage and climate indicators". *Energy and Buildings* 10: 81–86. doi:10.1016/0378-7788(87)90008-9.

Tahmasebi, F., R. Zach, M. Schuß, A. Mahdavi. 2012. "Simulation model calibration: An optimization-based approach". In: *Proceedings of BauSim 2012: Fourth German-Austrian IBPSA Conference*.

Wetter, M. 2009. *Generic Optimization Program User Manual Version 3.0.0*. Berkeley, U.S.A.: Lawrence Berkeley National Lab.

Zhdanov, M.S. 2002. *Geophysical inverse theory and regularization problems*. Amsterdam; The Netherlands: Elsevier.